



Cite this: *Soft Matter*, 2016, 12, 2501

Received 18th December 2015,
Accepted 5th February 2016

DOI: 10.1039/c5sm03066h

www.rsc.org/softmatter

Catalytically driven assembly of trisegmented metallic nanorods and polystyrene tracer particles†

Erik L. Jewell,^a Wei Wang^{*b} and Thomas E. Mallouk^{*a}

Trisegmented Au–Ru–Au and Ru–Au–Ru nanorods catalyze the decomposition of hydrogen peroxide, pumping fluid along their axis as “pullers” and “pushers” respectively. Numerical simulations and experiments with passive tracer particles show that catalytically generated hydrodynamic and electrostatic forces both contribute to pairwise and collective particle assembly.

Catalytic micromotors are mechano-chemical devices that are being increasingly studied for their emerging analytical and materials science applications, and for behavior that mimics aspects of biological motility.^{1–7} Powered colloidal objects can collectively assemble into dynamic structures that exist far from equilibrium, as so-called “active matter.” The elucidation of the pairwise and higher interactions of individual objects^{8–11} holds the key to better understanding this kind of collective behavior, which is already well studied and exploited in some devices for dense collections of bacterial swimmers.¹² Towards this end, we recently studied catalytically propelled bimetallic microrods, and found that electrostatic forces drive their assembly into staggered doublets and triplets, which have different modes of motion than isolated motors.¹³

While almost all of the work to date on catalytic micromotors has involved dipolar (*i.e.*, Janus) rods and particles with a well-defined propulsion direction, Davies Wykes *et al.* have recently studied rod-shaped particles in which the sequence of catalytic segments is A–B–A rather than A–B.¹⁴ The vector sum of forces on isolated rods of this type is zero, but they catalytically pump fluid inward or outward from their ends. These synthetic

swimmers are especially interesting because they mimic microbial head-actuated “pullers” such as *C. reinhardtii*, or “pushers,” such as *E. coli*, which swim by driving fluid away from their flagellar tails.^{15–17} Depending on the sequence of segments (A–B–A or B–A–B), catalytic trisegmented rods assemble into staggered bundles that act as rotors, or into T-shaped dimers that move as swimmers.¹⁴ A theoretical study by Pandey *et al.* has examined the collective behavior of filament structures (extensile or pusher, and contractile or pullers) driven solely by hydrodynamic forces at low Reynolds numbers.¹⁸ They noted, in addition to the formation of bundles and T-shapes, attractive interactions that drive extensile/pusher structures to form dense clusters at long times, and also tip-to-tip interactions of the contractile/puller filaments. Their model included short-range steric repulsion and hydrodynamic forces, but not the catalytically generated electric fields that are often important in bimetallic motor systems.

Here we report observations and finite-element numerical simulations of the pairwise interactions between trisegmented catalytic microrods (AuRuAu and RuAuRu) in hydrogen peroxide solutions. We find assembly patterns that include those observed by Davies Wykes *et al.*¹⁴ These patterns are shown by the simulations to be driven by both electrostatic and hydrodynamic forces. Additional experiments with charged tracer microparticles enable us to estimate the contribution of electrostatic forces, which are dominant at long distances, in driving the assembly of tracer particles with both pullers and pushers.

Tri-segmented microrods (composed of alternating segments of Au and Ru, ~4.5 μm long and ~300 nm in diameter) were grown using template-assisted electrodeposition as described previously (see ESI,† for experimental details).¹⁹ These microrods were suspended in unbuffered aqueous H₂O₂ solutions (0–10%) and were observed by using optical microscopy.

We synthesized RuAuRu and AuRuAu trisegmented microrods that would generate flow fields similar to those extensile (pusher) and contractile (puller) filaments, respectively. Earlier work has shown that H₂O₂ is preferentially oxidized and reduced, respectively, at the catalytic Au and Ru surfaces.^{19–21} The resulting imbalance in proton concentration creates an electric field around dipolar

^a Departments of Chemistry, Physics, and Biochemistry and Molecular Biology, The Pennsylvania State University, University Park, PA 16802, USA.
E-mail: tem5@psu.edu

^b School of Materials Science and Engineering, Shenzhen Graduate School, Harbin Institute of Technology, Shenzhen, 518055, China.
E-mail: weiwang_chem@126.com

† Electronic supplementary information (ESI) available: Experimental and computational methods, results of numerical simulations, optical images and videos (10 pp). See DOI: 10.1039/c5sm03066h

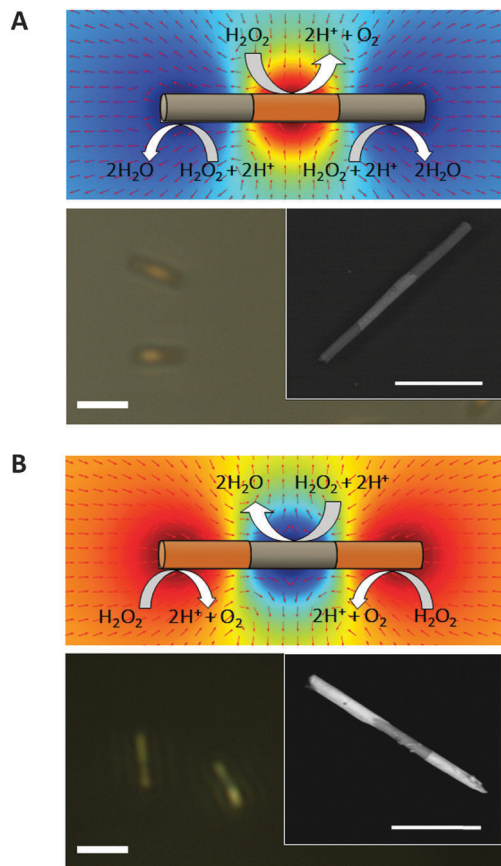


Fig. 1 (A) RuAuRu pushers and (B) AuRuAu pullers. Cartoons of trisegmented rods overlaid onto axisymmetric COMSOL numerical simulations, showing the electric field distribution and fluid flow lines arising from the catalytic decomposition of H_2O_2 . Red and blue shading represent positive and negative electric potential, respectively. Arrow sizes are not proportional to flow magnitude. Lower panels: optical micrographs with scanning electron micrograph insets showing the microrod structure; scale bars are $4\ \mu\text{m}$ and $2\ \mu\text{m}$, respectively.

AuRu rods, propelling the negatively charged rod in the direction of the Au end.

With a trimetallic rod, instead of a unidirectional flow, opposing flows are generated by catalytic decomposition of H_2O_2 . RuAuRu rods “push” fluid from the center to the tips (pusher, Fig. 1A) and thus draw in fluid at the center. Conversely, Au–Ru–Au rods “pull” fluid from the two tips towards the center, which by fluid continuity creates an outward flow from the center of the rod (puller, Fig. 1B). At the same time, the catalytically generated distribution of protons creates a quadrupolar electric field in the solution near the rod surface, which is opposite for pullers and pushers.

Fig. 2 illustrates that RuAuRu (pusher) rods in H_2O_2 form parallel doublets initially and then on longer timescales aggregate into dense bundles of parallel rods, in agreement with the predictions of Pandey *et al.*¹⁸ As noted by Davies Wykes *et al.*,¹⁴ the rods in these bundles are typically staggered rather than aligned tip-to-tip. We occasionally found other orientations of rods that were not anticipated based on earlier simulations and observations. These included dimers that crossed at the midpoint briefly before reorganizing, and also low number n -mers with two segments overlapping. On longer timescales massive

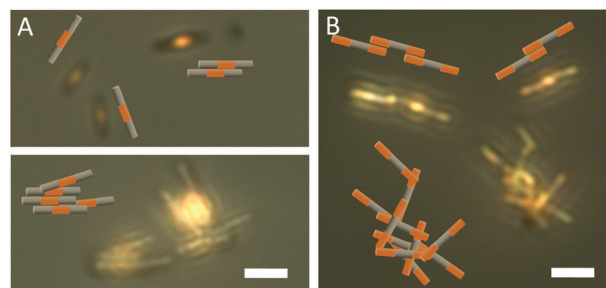


Fig. 2 Optical microscopy images showing aggregation behavior of (A) RuAuRu pushers and (B) AuRuAu pullers. In each image there are superimposed cartoons of the assemblies. Scale bars are $4\ \mu\text{m}$.

structures dominated and fewer monomers and dimers could be observed.

Our experiments with AuRuAu (puller) microrods also showed arrangements predicted by the simulations of Pandey *et al.*¹⁸ Specifically, we observed that pairs of AuRuAu rods did interact in a perpendicular fashion, but alignment was temporary and often the dimers would disassemble. When more than two rods interacted, aggregates began to form and continued to grow. These aggregates contained tip-to-tip connections as predicted, but in the form of parallel alignment in which Au ends overlapped by a single segment. This tip-to-tip alignment leads over time not to a dense bundle of parallel rods, but instead to more open clusters with random orientations of individual rods, as seen in the Fig. 2.

In order to better understand the interactions leading to the assembly of these structures, we established COMSOL models for both pushers and pullers interacting in different orientations. These axisymmetric and 2D multi-physics models explicitly included the diffusion of protons and counter-anions, the convection of fluid, and the electroosmotic pumping that occurs on the rod surface and drives the fluid motion.¹³ By examining the energy landscape of trisegmented rods in different pairwise configurations and comparing with experimental observations, we can begin to understand the relative roles of hydrodynamic and electrostatic forces in driving their assembly.

There are a number of ways two powered rods can approach each other and associate. We selected five of the most typical scenarios and examined the distributions of electrical potential and fluid pressure for both RuAuRu and AuRuAu. The results are presented in Fig. 3. By comparing simulations with experimental observations, we can conclude that the likelihood of observing each binding configuration is related to the relative strength of attractive and repulsive interactions. For example, two RuAuRu rods coming together into a completely parallel dimer (configuration 1 in Fig. 3) yields a very low fluid pressure between two rods, therefore favoring the association of the rods by hydrodynamic forces. While this configuration is frequently observed, the more common side-by-side dimer of pushers (configuration 2) pairs the central Au segments with Ru ends. For pushers, this arrangement creates a negative pressure between rods while minimizing electrostatic repulsion. The T-shaped arrangement of pushers (configuration 4) has weakly favorable pressure and electrostatic interactions, and is also frequently observed. Interestingly, pushers are never observed to pair by

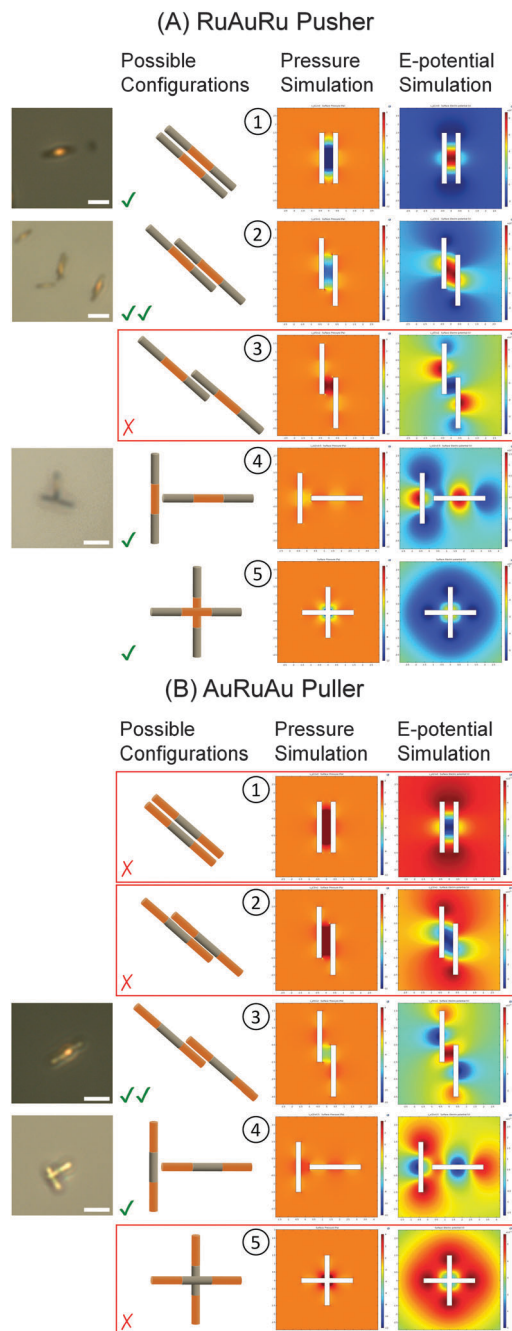


Fig. 3 Optical microscope images, 2D fluid pressure and electrical potential simulation results for dimer configurations of pusher and puller rods. Configurations (2) and (3) are the most frequently observed (marked with two green checkmarks) for pushers and pullers, respectively. Configurations with a high pressure are unfavorable and are not observed experimentally (marked with red X). Red and blue colors represent high and low fluid pressure in the “pressure simulation” column, respectively. Red and blue in the “E-potential simulation” column represent high and low electrical potential, respectively.

overlap of their end segments (configuration 3), which involves pressure and electrostatic interactions that are both repulsive. This configuration is in contrast the one that is most frequently observed for pullers, because of an attractive pressure interaction. Pullers do not associate in configurations (1), (2), or (5) because of repulsive pressure interactions. While the results of these 2D

simulations are not expected to be quantitatively accurate, the picture that emerges from them and from experimental observations is that while electrostatic forces contribute, hydrodynamic forces are dominant at short range in the association of pusher and puller rods.

In order to better understand the length scales of forces operative in this system, experiments were carried out using negatively charged 1 μm diameter polystyrene (PS) spheres. Electrostatic interactions should draw these negatively charged tracers to the Au segments of the rods, where catalytically generated H^+ ions create a positive potential near the rod surface. This is experimentally observed for both pushers and pullers, as shown in Fig. S1 (ESI †) for mixtures of spheres and rods of both kinds. The dynamics of these interactions are interesting and reveal something about the forces at work in the system. In the case of pushers (RuAuRu), negatively charged tracer particles should follow the catalytically generated flow lines and move towards the rods at the center. For AuRuAu pullers, the tracers should follow the flow lines along the rod axis as they approach the tips of the rods. Fig. 4 and Video S1 (ESI †) show an example of the latter trajectory, as three tracer particles sequentially approach the tip of an AuRuAu puller, ultimately forming a stable triangular cluster there. While the trajectory in the laboratory frame is complicated by Brownian rotation of the rod, the distance between the sphere centers and the Au tip of the rod decreases with time as they encounter each other within a distance of about 6–7 μm . Over the ~ 1 s period of this encounter, the sphere and rod tip move together at a relatively constant speed of about $10 \mu\text{m s}^{-1}$, corresponding to an attractive force (based on the drag coefficients of the rod and sphere^{13,20}) on the order of 0.1 pN.

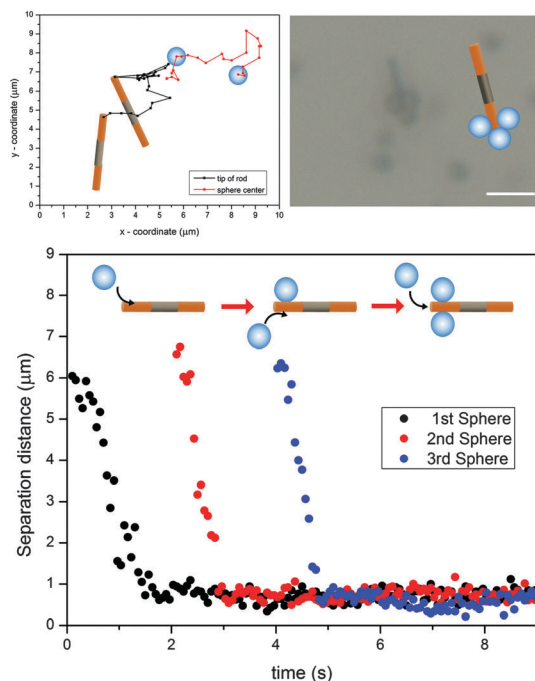


Fig. 4 Particle tracking and optical microscopy image showing the assembly of three PS spheres at the tip of an AuRuAu puller. Lower panel shows distance vs. time for the sequential approach of the spheres to the rod tip. Scale bar 4 μm .

Additional axisymmetric simulations were conducted in an effort to understand the balance of electrostatic and hydrodynamic forces in the rod-sphere assembly. In this case, isolated pullers and pushers were simulated and the electric potential and flow velocities were mapped as shown in Fig. 1. The fluid velocity and potential distribution around the rod were used to calculate the electroosmotic and electrophoretic contributions to the movement of tracer particles (1 μm diameter, zeta potential -63 mV) at different distances, and at different angles relative to the rod axis. The results are summarized in Fig. S2 and Table S1 (ESI†). The interesting trend that emerges from these simulations is that the electrophoretic component of tracer particle movement is dominant at all distances in the assembly of rods and passive tracers. In contrast, catalytically generated pressure forces are dominant in driving the assembly of pairs of pusher or puller rods.

In conclusion, RuAuRu and AuRuAu microrods behave as active pushers and pullers, respectively, when powered by the catalytic decomposition of H_2O_2 . At short distances (less than one rod length) the dominant forces that control assembly into pairs and larger aggregates are hydrodynamic, and aggregate shapes are consistent with the simulations of Pandey *et al.*¹⁸ However, the effects of electrostatic interactions are apparent in the staggered arrangement of “pusher” rod dimers, and become more important at increasing distances between particles. These electrostatic forces dominate the interactions of pusher and puller rods with passive tracer particles.

This work was supported by the National Science Foundation under MRSEC grant number DMR-1420620. WW is grateful for the financial support from National Natural Science Foundation of China (Grant No. 11402069) and government of Shenzhen (Grant No. KQCX20140521144102503).

Notes and references

- 1 W. Wang, W. Duan, S. Ahmed, A. Sen and T. E. Mallouk, *Acc. Chem. Res.*, 2015, **48**, 1938–1946.
- 2 S. Sanchez, L. Soler and J. Katuri, *Angew. Chem.*, 2015, **54**, 1414–1444.
- 3 M. Gui, C. C. Mayorga-Martinez and A. Merkoj, *Chem. Rev.*, 2014, **114**, 6285–6322.
- 4 H. Wong and M. Pumera, *Chem. Rev.*, 2015, **115**, 8704–8735.
- 5 J. R. Howse, R. A. L. Jones, A. J. Ryan, T. Gough, R. Vafabakhsh and R. Golestanian, *Phys. Rev. Lett.*, 2007, **99**, 048102.
- 6 S. Tottori, L. Zhang, K. E. Peyer and B. J. Nelson, *Nano Lett.*, 2013, **13**, 4263–4268.
- 7 W. Gao, A. Pei, X. Feng, C. Hennessy and J. Wang, *J. Am. Chem. Soc.*, 2013, **135**, 998–1001.
- 8 N. Sharifi-Mood, A. Mozaffari, U. Córdova-Figueroa, 2015, arXiv:1510.03000.
- 9 J. Schwarz-Linek, C. Valeriani, A. Cacciuto, M. E. Cates, D. Marenduzzo, A. N. Morozov and W. C. K. Poon, *Proc. Natl. Acad. Sci. U. S. A.*, 2012, **109**, 4052–4057.
- 10 R. Soto and R. Golestanian, *Phys. Rev. Lett.*, 2014, **112**, 068301.
- 11 S. Ahmed, D. Gentekos, C. A. Fink and T. E. Mallouk, *ACS Nano*, 2014, **8**, 11053–11060.
- 12 A. Sokolov, M. M. Apodaca, B. A. Grzybowski and I. S. Aranson, *Proc. Natl. Acad. Sci. U. S. A.*, 2009, **107**, 969–974.
- 13 W. Wang, W. Duan, A. Sen and T. E. Mallouk, *Proc. Natl. Acad. Sci. U. S. A.*, 2013, **110**, 17744–17749.
- 14 M. S. Davies Wykes, J. Palacci, T. Adachi, L. Ristroph, X. Zhong, M. D. Ward, J. Zhang, M. J. Shelley, 2015, arXiv:1509.06330v1.
- 15 D. Saintillan and M. J. Shelley, *Phys. Rev. Lett.*, 2008, **100**, 178103.
- 16 E. Lauga and T. R. Powers, *Rep. Prog. Phys.*, 2009, **72**, 096601.
- 17 D. Saintillan and M. J. Shelley, Theory of active suspensions, in *Complex Fluids in Biological Systems*, ed. S. Spagnolie, Springer, 2015, pp. 319–355.
- 18 A. Pandey, P. B. Sunil Kumar, R. Adhikari, 2015, arXiv:1408.0433v1.
- 19 Y. Wang, R. M. Hernandez, D. J. Bartlett, J. M. Bingham, T. R. Kline, A. Sen and T. E. Mallouk, *Langmuir*, 2006, **22**, 10451–10456.
- 20 W. Wang, T.-Y. Chiang, D. Velegol and T. E. Mallouk, *J. Am. Chem. Soc.*, 2013, **135**, 10557–10565.
- 21 A. Nourhani, P. E. Lammert, V. H. Crespi and A. Borhan, *Phys. Fluids*, 2015, **27**, 012001.